Journal of The Electrochemical Society, **161** (3) A326-A329 (2014)
0013-4651/2014/161(3)/A326/4/$31.00 © The Electrochemical Society

Influence of Different Electrolyte Concentrations on the Performance of an AB_2-Type Alloy

P. S. Martínez,[a] F. C. Ruiz,[a,b,z] and A. Visintin[b,c,*]

[a] *Centro Atómico Bariloche (CAB) - Comisión Nacional de Energía Atómica (CNEA), C. P.: 8400 S. C. de Bariloche (RN), Argentina*
[b] *CONICET Consejo Nacional de Investigaciones Científicas y Técnicas, C1033AAJ Ciudad de Buenos Aires, Argentina*
[c] *Instituto de Investigaciones Fisicoquímicas, Teóricas y Aplicadas, Universidad Nacional de La Plata, Comisión de Investigaciones Científicas Provincia de Buenos Aires (C.I.C.), CP: 1900 La Plata, Argentina*

A systematic study about the effect of different electrolyte concentrations (KOH 2M, 4M, 6M and 8M) at 293 K on the electrochemical properties of $Ti_{12}Zr_{21.5}V_{10}Ni_{38.4}Cr_{4.5}Mn_{13.6}$ AB_2-type alloy was performed. This alloy can be used as active material of the negative electrode of nickel-metal hydride batteries. The variation in KOH concentration has influence in the activation processes, the discharge capacity and the cycle life of the AB_2 alloy. The maximum discharge capacity and the faster activation are reached at KOH 8M, whereas the better cycle life performance is achieved to KOH 4M. These are innovative results because previous research has not explicitly considered the type and composition of the studied alloy.
 [DOI: 10.1149/2.042403jes]

Manuscript submitted August 22, 2013; revised manuscript received October 28, 2013. Published December 27, 2013.

The global rechargeable battery market is expected to exhibit strong growth in the next years, due to their use in large amount and diversity of portable electronic devices, electric and hybrids vehicles, toys, robots, etc.[1–7] Nickel-metal hydride (Ni-MH) batteries belongs to this kind of accumulators. Ni-MH batteries have been extensively studied owing to their high capacities, fast charge and discharge capabilities, environment-friendly features and long cycle life.[8–12]

The negative electrode of Ni-MH battery is constituted by a hydride-forming alloy and it is the most studied component in these batteries.[13,14] The alloy/electrolyte interaction is very important due to the fact that the alloy components suffer from corrosion processes generated by the high KOH concentration.[15,16]

The ionic conductivity of KOH is the highest in 8M concentration at 293 K.[17] In this molar concentration, the electrolyte promotes a severe corrosion issue on some alloys .There are a few works about the effect of the electrolyte concentration on the properties of hydride forming alloys for NiMH batteries. Khaldi et al. showed better electrochemical properties using KOH 1M instead of KOH 8M on an AB_5 alloy, e. g. reduction of loss of capacity, lower polarization and lower thickness of the corrosion layer.[18] Guiose et al.[19] studied the role of the electrolyte concentration (KOH 6 and 8M) in the activation and degradation of an ABalloy. The increase of KOH concentration causes, on one hand a fast activation, on the other hand a higher loss of the capacity. Zhang et al.[20] studied the effect of KOH 5, 6, 7, 8 and 9M on the electrochemical properties at low temperatures (233 K) of the $LaNi_5$ alloy, obtaining the highest discharge capacity and discharge voltage plateau at KOH 6M. Song et al.[21] studied this influence in the oxide $LaCrO_3$ perovskite-type employing KOH electrolyte in the 5.6 −12.5 M range, finding that capacity increases as KOH concentration is augmented. In a previous work,[22] we have investigated different KOH concentrations on an AB_5 alloy.

Table I shows a summary of the results obtained in the cited articles.

This article presents a systematic study about the effect of KOH concentration (2, 4, 6 and 8M) on electrochemical properties of an AB_2 alloy.

The alloy composition is $Ti_{12}Zr_{21.5}V_{10}Ni_{38.4}Cr_{4.5}Mn_{13.6}$. Besides the fact that there are few publications on this specific topic, this investigation is novel in terms of the alloy composition and type, the systematic method used and the analyzed electrolyte concentrations.

X-ray diffraction (XRD) technique has been used to verify the crystalline structure. Electrochemical studies included measurements of charge/discharge cycles, high-rate dischargeability (HRD) and electrochemical impedance spectroscopy (EIS).

Experimental

An AB_2 alloy of target composition $Ti_{12}Zr_{21.5}V_{10}Ni_{38.4}Cr_{4.5}Mn_{13.6}$ was obtained by melting the components in an electric arc furnace inside a copper-cooled heart, with tungsten electrode and under argon atmosphere (99,998%). In order to improve the purity of the melting atmosphere, a sacrifice button of Zr was melted previously. The resulting alloy button was turned over and remelted at least two times to assure homogeneity.

In order to identify the crystal structure of the alloy, the X-ray diffraction technique (Cu Kα radiation) was conducted.

For the electrochemical measurements, metal hydride electrode has used as a working electrode, a nickel mesh as a counter electrode, and mercury/mercury oxide electrode (Hg/HgO) as a reference electrode.

The electrodes were prepared by compacting a mixture of 100 mg of alloy powders (74 μm < size particle < 125 μm) and 100 mg of teflonized carbon (Vulcan XC-72). A Ni mesh connected to a Ni wire was used as current colector. The mixture and the Ni mesh were compacted to a pressure of 1900 kg/cm^2 at room temperature.

For the electrochemical tests, the electrodes were charged at a current density of 100 mA/g for 4.5 h and discharged at 100 mA/g until the cutoff potential of −0.6 V vs. Hg/HgO was reached.

The electrochemical measurements were carried out using four electrochemical cells containing different solutions (KOH 2M, 4M, 6M and 8M) at 293 K

For HRD measurements, different values of discharge current densities were used.

EIS experiments were performed at 50% state of charge (SOC). In the course of this analysis, the frequency region from 65 kHz to 0.5 mHz was scanned and the ac amplitude used was 6 mV.

EIS and HRD measurements were performed when the maximum capacity was reached in an Autolab PGSTAT 30 potentiostat/galvanostat.

Results and Discussion

The crystal structure of $Ti_{12}Zr_{21.5}V_{10}Ni_{38.4}Cr_{4.5}Mn_{13.6}$ alloy was investigated by XRD analysis. Fig. 1 shows the X-ray diffraction pattern of the multi-component AB_2 alloy. As can be seen, the $Ti_{12}Zr_{21.5}V_{10}Ni_{38.4}Cr_{4.5}Mn_{13.6}$ alloy crystallizes in the hexagonal structure C14 Laves phase. Small additional peaks found correspond to a $ZrNi_3$ compound. The lattice constants, a and c, were calculated from XRD patterns, obtaining the following values: $a = 4.954$ Å, $c = 8.077$ Å.

The dependence of the discharge capacity on the cycle number is shown in Figure 2 for all KOH concentrations, at discharge current density of 100 mA/g.

*Electrochemical Society Active Member.
[z]E-mail: ruizfabricio@yahoo.com.ar

Table I. Summary of obtained results on articles based in KOH electrolyte concentration.

Article	Alloy/studied [KOH]	C (mAh/g)	Act. (number of cycles)	Effect of [KOH] increment on cycle life	HRD	R_{ct}	R_{ohm}	D_H
Khaldi[18]	$LaNi_{3.55}Mn_{0.4}Al_{0.3}Co_{0.75}$ (AB_5) 1M and 8M	295 (1M) 237 (8M)	No significant difference	Negative	–	1.7 Ω (1M) 1.2 Ω (8M)	1.3 Ω (1M) 2.5 Ω (8M)	–
Guiose[19]	$Ti_{0.66}Zr_{0.36}Ni_{0.98}$ (≈ AB) 6M and 8M	230 (6M) 335 (8M)	20 (6M) 4 (8M)	Negative	–	–	–	–
Zhang[20]	$LaNi_5$ (AB_5) 5M to 9M	All ≈ 235	–	–	Maximum at 6M	Constant	–	Maximum at 6M
Song[21]	$LaCrO_3$ (≈ AB_4) 5.6M to 12.5M	Max. 125 (12.5M)	–	–	–	Decreases with the KOH concentration increases.	–	Constant
Ruiz[22]	$LaNi_{3.55}Mn_{0.4}Al_{0.3}Co_{0.75}$ (AB_5) 2M to 8M	Max. 325 (6M and 8M)	Minimum at 8M	Negative	Maximum at 6M	Minimum at 6M	Minimum at 6M	Constant

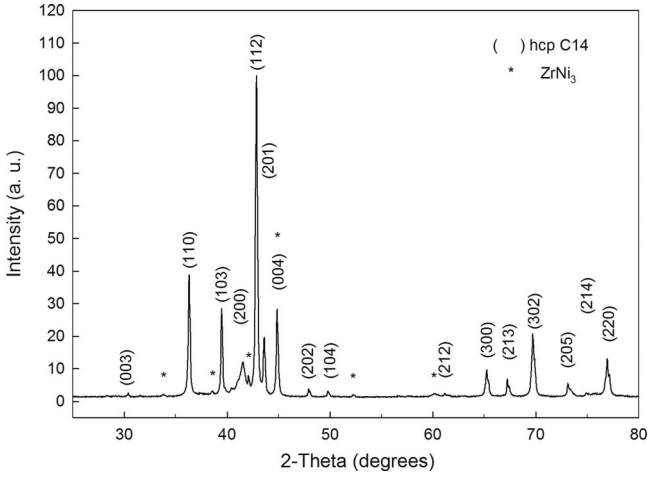

Figure 1. $Ti_{12}Zr_{21.5}V_{10}Ni_{38.4}Cr_{4.5}Mn_{13.6}$ alloy XRD pattern.

It can be seen that increasing KOH concentration leads to a significant improvement in the activation property of the electrodes and a maximum discharge capacity value (Fig. 3).

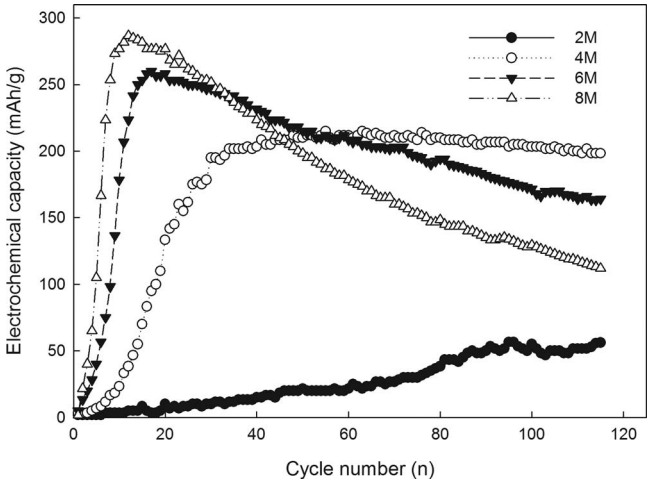

Figure 2. Electrochemical discharge capacity of $Ti_{12}Zr_{21.5}V_{10}Ni_{38.4}Cr_{4.5}Mn_{13.6}$ at different KOH concentrations.

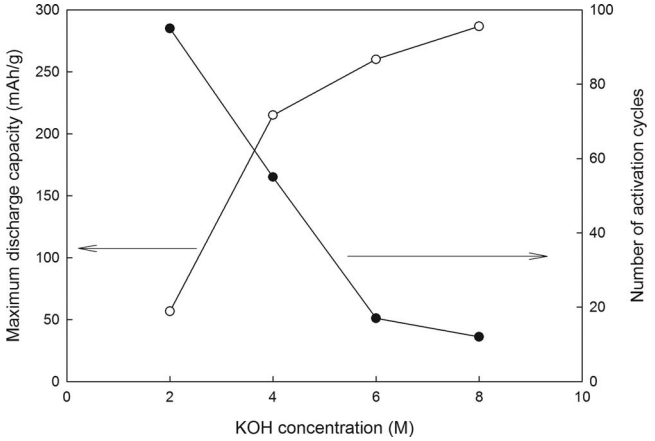

Figure 3. Maximum discharge capacity (left) and number of activation cycles (right) vs. KOH concentration.

The maximum discharge capacity obtained was 287 mAh/g, corresponding to KOH 8M. On the other hand, the increase of KOH concentration affects the cycle life in a negative way Table II shows the values corresponding to the variation of the discharge capacity per cycle.

These values were obtained from the slope of the linear part of the capacity curve, taking the cycle corresponding to the maximum capacity as a starting point.

In Figure 4, it can be seen the HRD measurements, in absolute and relative capacity values for all samples. The best HRD performance corresponds to KOH 8M, followed by 6, 4 and 2M.

Table II. Variation of the discharge capacity per cycle for all samples.

KOH concentration (M)	Variation of the capacity [(mAh/g)/cycle]
2	−0.06
4	−0.28
6	−0.92
8	−1.70

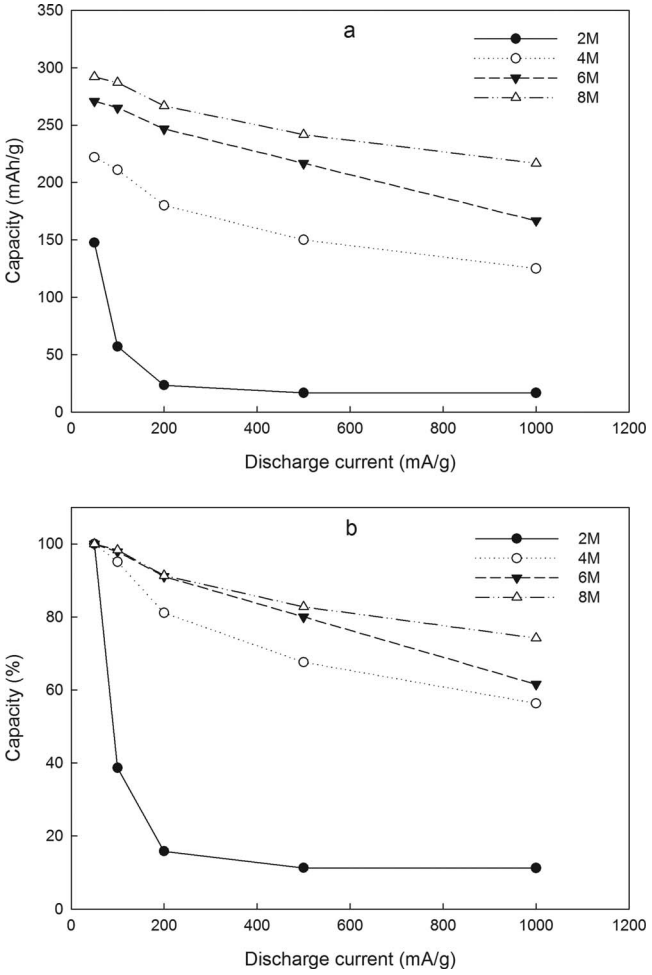

Figure 4. HRD measurements of all samples, in absolute (a) and relative (b) values.

The impedance plot of all electrodes is shown in the Figure 5, presenting an enlarged view of this plot in Figure 6.

All these spectra consist of two semicircles in the high and low frequency regions. The small semicircle in the high frequency region generally is associated to the contact resistance between the alloy particles and the current collector[23,24] but this association is not clear.

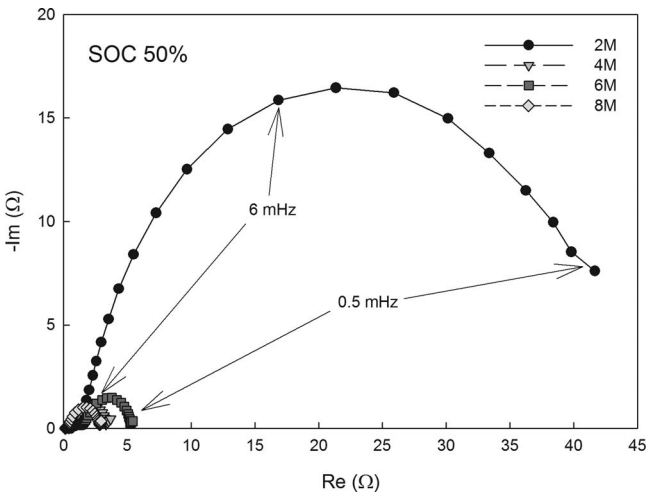

Figure 5. Nyquist plot corresponding to 2, 4, 6 and 8M KOH concentration.

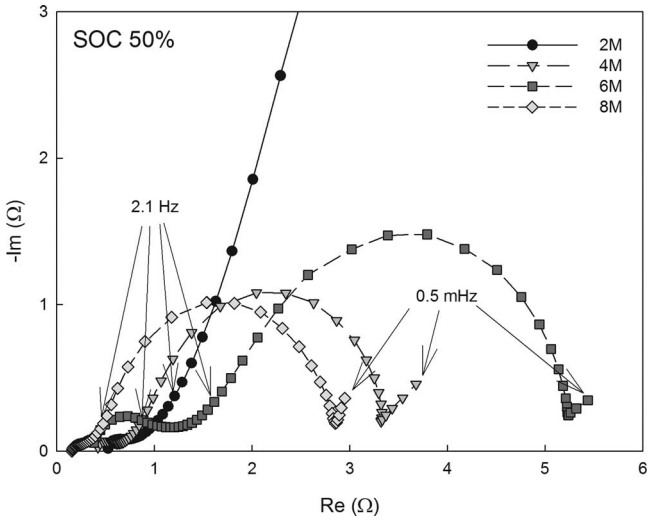

Figure 6. Nyquist plot of 4, 6 and 8M KOH concentration (magnification of Figure 5).

The second arc is attributed to the charge transfer resistance (R_{ct}). In 4, 6 and 8M spectra, it can be seen a linear part corresponding to Warburg impedance. The ohmic resistance decreases as increases the KOH concentration (Table III).

The charge transfer resistance of KOH 2M is very high in relation to the other samples. The R_{ct} values of 4, 6 and 8M are similar among them.

It is evident that the electrolyte concentration affects the capacity, the cycle life, the HRD performance and the activation processes. As can be seen in Table I, in all the cited articles (except Khaldi et. al.) the maximum value of the discharge capacity is achieved to maximum KOH concentration. Also, cycle life is affected in a negative way. The other properties exhibit different results.

According to See et al,[17] electrolyte conductivity values at 293 K were calculated, obtaining the following data: 0.390 S/cm^2 (2M), 0.490 S/cm^2 (4M), 0.566 S/cm^2 (6M) and 0.580 S/cm^2 (8M). The activation processes and the HRD performance are related to kinetic processes, which are influenced, in part, by the electrolyte conductivity. In the case of 2M KOH, the decrease in conductivity strongly affects the charge transfer resistance.

On the other hand, the cycle life gets worse as KOH concentration increases. The discharge capacity degradation with charge/discharge cycling related to KOH concentration, can be explained by diverse causes such as formation of surface barriers that makes difficult the charge transfer between the active material and the electrolyte, loss of active material by oxidation reactions and loss of electrical contact between alloy particles by pulverization. This effects are favored to a high KOH concentration. In particular, it is well known that the AB_2 type alloys have a short cycle life, which is ascribed to a low resistance corrosion and formation of a surface oxide layer.[25]

In summary, in our previous work about the effect of KOH concentration on electrochemical properties of AB_5 alloy,[22] it was found that the 6M and 8M KOH exhibit the maximum discharge capacity and the best HRD performance. Also, the capacity loss rate increases with increasing KOH concentration. In the present work, similar effects are observed, but the cycle life of AB_2 alloy is more sensible

Table III. Relationship between the ohmic and charge transfer resistances with KOH concentration.

KOH (M)	2	4	6	8
R_{ohm} (Ω)	0.52	0.41	0.38	0.15
R_{ct} (Ω)	46	2.47	3.75	2.43

to the KOH concentration. It could be closely related to the different elements which constitute the AB2 and AB5 composition.

Conclusions

The effect of the KOH concentration on the electrochemical properties of $Ti_{12}Zr_{21.5}V_{10}Ni_{38.4}Cr_{4.5}Mn_{13.6}$ AB_2-type alloy has been studied through different electrochemical techniques.

The increase of KOH concentration causes:

- Increase of the maximum discharge capacity value.
- Improves both the activation and the HRD performance.
- Increase the capacity loss during cycling.
- Decrease of the ohmic resistance.

In particular, the cycle life of this AB_2 alloy is strongly affected by the variation of KOH concentration.

References

1. W. Jiang, C. Qin, R. Zhu, and J. Guo, *J Alloy Compd.*, **565**, 37 (2013).
2. J. Zhang, Y. Zhu, Y. Wang, Z. Pu, and L. Li, *Int J Hydrogen Energy*, **37**, 18140 (2012).
3. W. Shen, S. Han, Y. Li, J. Yang, and K. Xiao, *Materials Chemistry and Physics*, **132**, 852 (2012).
4. Y. Zhang, B. Li, Y. Cai, X. Dong, J. Ren, and X. Wang, *Materials Science and Engineering: A*, **458**, 67 (2007).
5. D. J. Cuscueta, H. L. Corso, A. Arenillas, P. S. Martinez, A. A. Ghilarducci, and H. R. Salva, *Int J Hydrogen Energy*, **37**, 14978 (2012).
6. A. Ledovskikh, D. Danilov, P. Vermeulen, and P. H. L. Notten. *J. Electrochem. Soc.*, **157**, A861 (2010).
7. K. Young, T. Ouchi, B. Huang, B. Reichman, and M. A. Fetcenko, *J Power Sources*, **196**, 8815 (2011).
8. M. Tliha, S. Boussami, H. Mathlouthi, J. Lamloumi, and A. Percheron-Guégan., *Materials Science and Engineering: B*, **175**, 60 (2010).
9. S. Li, M. Zhao, J. Zhai, and F. Wang, *Materials Chemistry and Physics*, **113**, 96 (2009).
10. X. Dong, F. Lü, Y. Zhang, L. Yang, and X. Wang, *Materials Chemistry and Physics*, **108**, 251 (2008).
11. S. Li, M. Zhao, L. Wang, Y. Liu, and Y. Wang. *Materials Science and Engineering: B*, **150**, 168 (2008).
12. P. Piela, Z. Rogulski, M. Krebs, E. Pytlik, M. Schmalz, J. Dłubak, M. Karwowska, A. Gumkowska, and A. Czerwiński, *J. Electrochem. Soc.*, **157**, A254 (2010).
13. T.-K. Ying, X.-P. Gao, W.-K. Hu, F. Wu, and D. Noréus, *International Journal of Hydrogen Energy*, **31**, 525 (2006).
14. X. Zhang, Y. Chai, W. Yin, and M. Zhao, *Journal of Solid State Chemistry*, **177**, 2373 (2004).
15. J. S. Kim, C. H. Paik, W. I. Cho, B. W. Cho, K. S. Yun, and S. J. Kim, *Journal of Power Sources*, **75**, 1 (1998).
16. B. H. Liu, Z. P. Li, Y. Matsuyama, R. Kitani, and S. Suda, *J. Alloy Compd.*, **296**, 201 (2000).
17. D. M. See and R. E. White, *J Chem Eng Data*, **42**, 1266 (1997).
18. C. Khaldi, H. Mathlouthi, and J. Lamloumi, *J Alloy Compd*, **469**, 464 (2009).
19. B. Guiose, F. Cuevas, B. Décamps, E. Leroy, and A. Percheron-Guégan, *Electrochim Acta*, **54**, 2781 (2009).
20. X. Zhang, Y. Chen, M. Tao, and C. Wu, *J Rare Earth*, **26**, 402 (2008).
21. M. Song, Y. Chen, M. Tao, C. Wu, D. Zhu, and H. Yang, *Electrochim Acta*, **55**, 3103 (2010).
22. F. C. Ruiz, P. S. Martínez, E. B. Castro, R. Humana, H. A. Peretti, and A. Visintin, *International Journal of Hydrogen Energy*, **38**, 240 (2013).
23. N. Kuriyama, T. Sakai, H. Miyamura, I. Uehara, H. Ishikawa, and T. J. Iwasaki, *J. Electrochem. Soc.*, **139**, L72 (1992).
24. X. Zhao, L. Ma, M. Yang, Y. Ding, and Y Shen, *Int J Hydrogen Energy*, **35**, 3076 (2010).
25. K. Young, J. Nei, B. Huang, and M. A. Fetcenko, *Int J Hydrogen Energy*, **36**, 11146 (2011).